

# 통합적 광추적 모델에 의한 해양탐재체 GOCI의 궤도 상 광학 성능 검증

함선정\*, \*\*, 이재민\*, 김성희\*\*, 윤형식\*\*, 강금실\*\*, 명환춘\*\*, 김석환\*

## Integrated Ray Tracing Model for In-Orbit Optical Performance Simulation for GOCI

Sun-Jeong Ham\*, \*\*, Jae Min Lee\*, Seonghui Kim\*\*, Heong Sik Youn\*\*, Gm Sil Kang\*\*,  
Hwan Chun Myung\*\* and Sug-Whan Kim\*

### 요 약

현재 항공우주연구원은 2008년에 발사 운용 예정인 통신-해양-기상위성의 주요 탑재체들 중의 하나로 한반도 주변 해역의 환경 상태를 정밀 측정하려는 정지궤도 해색센서(GOCI)를 개발하고 있다. 본 논문에서는 해색센서의 궤도상 임무성능 검증을 원활히 수행하기 위해 통합적 광선 추적 기법을 이용한 임무성능 검증 수치모사 모델을 개발 제시한다. 수치모사 모델 내에서 태양은 지구 방향으로 복사에너지를 방사하는 구형 광원으로 입력되었고, 구면인 지구 표면 중 한반도를 중심으로 한 2500km x 2500km 넓이의 곡면 관측 영역은 지표와 해수면으로 구분하여 서로 다른 특성의 람버트 산란 면들로 정의되었다. 수치모사 모델 내에서 해색센서 광학시스템은 태양을 출발하여, 지표 및 해수면의 환경적 특성 변화를 반영하는 반사도의 변화에 따라 산란 후 입사되어오는 광선들의 경로를 추적하여 초점면 광소자에 멩히게 하여준다. 이러한 통합적 광선 추적 기법을 이용하여 개발 중인 해색센서가 궤도상에서 한반도 동남부 연해 상에서 가장적으로 발생된 반사율 감소 0.014에 해당하는 적조현상을 탐지 해낼 수 있음을 수치모사 입증하였다. 이 같은 결과는 본 논문에 기술된 통합적 광선 추적 기법을 이용한 과학임무 성능 검증 수치모사 모형은 해색센서 뿐만 아니라, 다른 과학적 측정 목적의 위성 탑재체의 임무성능 검증에도 활용 할 수 있는 기반 기술을 확립하였다는 의의를 제공한다.

### ABSTRACT

GOCI (Geostationary Ocean Color Imager) is one of the three COMS payloads that KARI is currently developing and scheduled to be in operation from around 2008. Its primary objective is to monitor the Korean coastal water environmental condition. We report the current progress in development of the integrated optical model as one of the key analysis tools for the GOCI in-orbit performance verification. The model includes the Sun as the emitting light source. The curved Earth surface section of 2500 km x 2500 km including the Korean peninsular is defined as a Lambertian scattering surface consisted of land and sea surfaces. From its geostationary orbit, the GOCI optical system observes the reflected light from the surfaces with varying reflectance representing the changes in its environmental conditions. The optical ray tracing technique was used to demonstrate the GOCI in-orbit performances such as red tide detection. The computational concept, simulation results and its implications to the on-going development of GOCI are presented.

**Key Words** : optical model, GOCI, ray-tracing technique, in-orbit performance

\* Sat\*SOL. Dept. of Astronomy and Space Science, Yonsei University Sin Chon-dong Seodaemun-gu, Seoul, KOREA  
Email: redion81@gmail.com

\*\*Korea Aerospace Research Institute 45 Eoeun-dong Yuseong-gu Daejeon Korea Email: youn@kari.re.kr, redion81@kari.re.kr

## 1. Introduction

With the advancement of space technology over the last few decades, ocean color measurement has been one of the key earth environmental monitoring programs from the space. Up until today, the majority of space ocean color data has been collected from the sensors at the low earth polar orbit (LEO). Examples of the current generation sensor (or missions) may include, but not limited to, MODIS[1], MERIS[2] and COCTS (HY-1)[3]. The common characteristics of these sensors is the narrow swath of less than or around 2000 Km, providing the ground resolution range of around few hundred meters to, typically, one kilometers.

As opposed to such existing LEO sensors, the new generation sensors of a wider FOV with the comparable ground resolution are being developed for ocean environment monitoring from the geostationary earth orbit. Examples include HES-CW[4] and GOCI[5]. In particular, GOCI is one of the three main payloads for the COMS satellite that Korea Aerospace Research Institute is currently developing in collaboration with Astrium. As of today, the GOCI development activity is progressing on schedule. The manufacturing phase will begin just after the project critical design review scheduled around February 2006.

In preparation of the in-orbit calibration following the ground calibration and integration/test activity, an instrument end-to-end performance simulation tool needs to be developed prior to the integration phase. Here in this paper, we report the current development status of a new 3D GOCI optical system model and the integrated end-to-end performance analysis technique based on optical ray tracing. We then demonstrated, whilst it is still in early phase, its usefulness by applying it for the red tide detection.

## 2. GOCI optical model verification

### 2.1. GOCI payload requirement

The key optical system requirements of GOCI are summarized in Table. 1 below. The three mirror anastigmatic (TMA) design was used for the instrument optical system configuration, providing the balanced trade-off between the optical train length and the instrument packaging space.

Table. 1. GOCI optical system requirement

Pupil diameter	140mm	F - number	8.36
Focal length	1171mm	Channels	8
Total FOV	5300× 5300 pixels	Nyquist frequency	43.4mm-1 (NS) 33.8mm-1 (EW)
Detector size	1415× 1432 (14.81μm ×11.53μm)	MTF	> 27.8% (NS, B5) > 35.8% (EW, B5)

### 2.2 GOCI optical model

As shown in Fig. 1, the GOCI optical train begins with a front end scan mirror that relays the incident light to the primary mirror (M1) and expands the measurement target area from mere 1.03 degree(EW) to about 4 degree with the motorized scan mechanism. This can be achieved by combining 16 (i.e. 4 by 4) snap shot images of 1.03 × 1.03 degree in instant field of view (IFOV). After the scan mirror, the light passes through the aperture stop, heading to the primary mirror (M1). The reflected light from M1 is then further reflected three times via the secondary mirror (M2), the tertiary mirror (M3) and then the folding mirror, before passing through the filter assembly. The incident light is then finally arrived at the focal plane where a CMOS Imager Sensor(CIS) chip surface is positioned after the detector window.

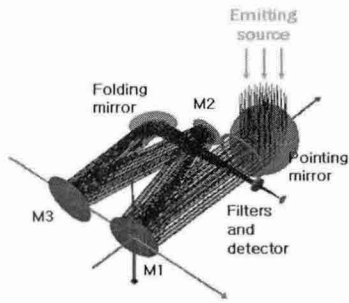


Fig. 1. GOCI optical model translated from the original design by Bevillon & Archer. [6]

### 2.3 Design performance verification

The original GOCI optical design proposed by Bevillon & Archer[6] was translated to re-construct the new 3D optical design of GOCI that can be incorporated into the integrated end-to-end ray tracing model discussed in the following section. The re-constructed GOCI optical model was materialized in the ASAP optical analysis environment [7]. Figure 2 show the spot diagrams of the original design and of the re-constructed model, exhibiting almost identical imaging performance.

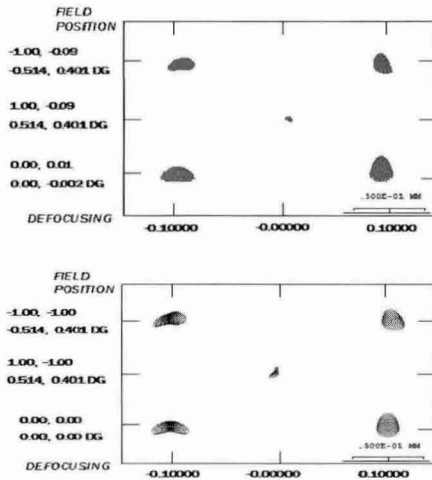


Fig. 2. Spot diagrams of the original design (left) and of the reconstructed design (right)

In addition, Fig.3 presents the modulation transfer function (MTF) at the Nyquist frequency plotted against the wavelength. We note that there are two MTF plots available from the original design. The MTF plot (magenta square) is obtained from the original GOCI optical design

with the single element filter configuration, whilst the MTF plot (blue line) comes from the original GOCI optical design of the improved (two elements) filter sub-system. It is worth noting that the re-constructed GOCI design (using ASAP) uses the two element filter sub-system and, hence, its MTF plot appears to be similar to that (magenta square symbol) of the two element filter design.

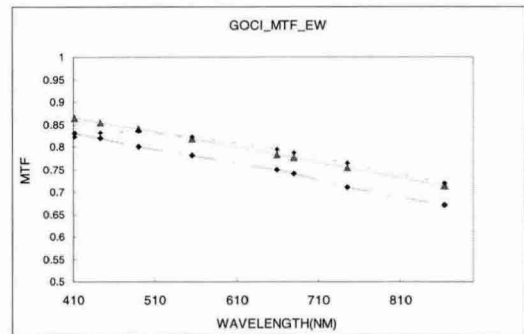
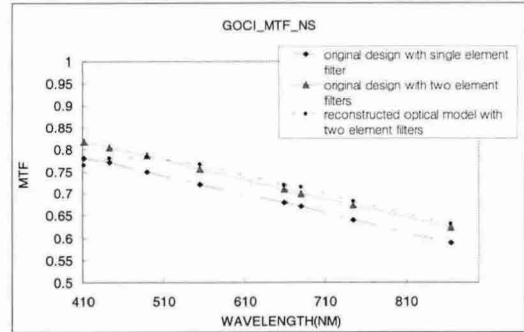


Fig. 3. MTF plots at Nyquist frequency versus wavelength. The top graph shows E-W MTF, while the bottom is for N-S MTF. All MTF values prove that the GOCI optical designs presented here meet the MTF requirement successfully. [8]

The assessment of imaging performance of the re-constructed GOCI optical system in terms of spot diagram and MTF supports its validity that it can be imported into the integrated ray tracing model described in the following subsection.

### 2.4. Integrated end-to-end GOCI optical model

Having proved designed optical performance in the previous section, the re-constructed GOCI optical model was then incorporated into the integrated end-to-end ray tracing model as shown in Fig. 4. The model includes the sun defined as an emitting disk from which the light rays emit

toward the earth. A curved section of the earth's surface including the observation target of 2500 × 2500 km<sup>2</sup> was modeled as the Lambertian scattering surface that reflects the incident rays. The target area is composed of 16 tiles each of which corresponds to the instant field of view of GOCI. The tiles have the area of high reflectance of 0.3 representing the land and of the low reflectance of around 0.055 for the clear ocean surface. A part of scattered light rays from the target area are sent to the GOCI aperture at the geostationary orbit. The rays arriving at the instrument entrance aperture travel through the optical train and focused at the detector plane.

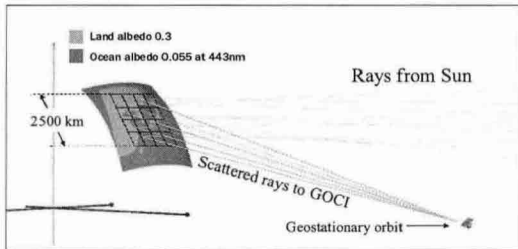


Fig. 4. Integrated end-to-end optical ray tracing model including the sun, the earth and GOCI

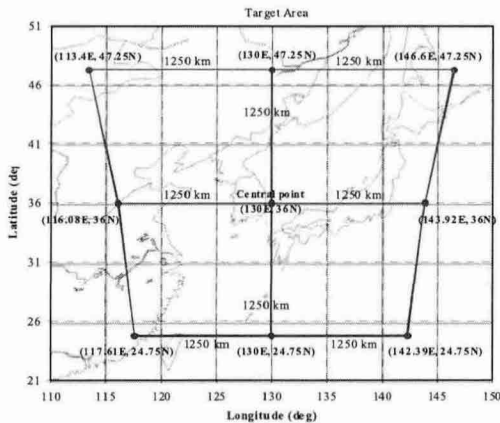


Fig. 5. GOCI observation coverage of about 4 × 4 deg in total. It consists of 16 tiles of 1 deg IFOV. Using 16 sequential scanning steps from bottom-left to top-left GOCI will detect 2500 × 2500 km<sup>2</sup> area around the Korean peninsula.

The target area of 2500 × 2500 km<sup>2</sup> as seen by the GOCI focal plane is shown in Fig.5. The 4 × 4 rectangular grids are distorted and this is

caused by the geometric configuration between the curved target area and the GOCI observation location at the geostationary orbit. When the in-orbit operation is performed, each observation tile is selected, one by one, by employing the scan mirror mechanism in sequence.

### 3. GOCI in-orbit performance

#### 3.1. Demonstration of input flux correction

As far as the isolated GOCI instrument is concerned, the typical radiometric calibration is to characterize the detector response to the incident flux at the image plane. It uses either a simple linear equation or a second order quadratic equation that relates the flux read from the detector pixel to the absolute radiance obtained from the calibration source.

In end-to-end ray tracing simulation, it is necessary to devise the way to estimate the incident flux at the entrance aperture from the flux registered at the detector plane. This requires the calculation method similar to the calibration process.

Thus, we demonstrate the feasibility of using the ray tracing simulation for the calibration by establishing the first order linear equation that relates the detector plane flux to the incident flux at the entrance aperture. This estimation takes into account the resulting effect from the variation of light scattering characteristics among the observation tiles, as the angles of incident and reflected lights varies even in single measurement run covering the 16 tiles.

First, equation 1 [9] was used to estimate the incident flux at the entrance aperture received from each tile.

$$F_{sc} = F_i \cdot \rho(\theta_i, \phi_i; \theta_s, \phi_s) \frac{A \cos \theta_e \cos \theta_s}{R^2} \quad \text{Eq. (1)}$$

where  $F_i$  is the incident flux on a slot,  $\rho$  BRDF of a slot,  $A$  the sampling area,  $\theta$  and  $\phi$  are polar and azimuth angles, and the subscription e and s are scatter angle and the angle between

scattered ray and sampling edge normal.[9]. Eq. 1 yields the reference flux to which the simulated (i.e. ray traced) flux at the detector plane is to be corrected. For example the incident flux at the entrance aperture from the tile 10 was computed as  $1.335 \times 10^{-4}$  watt and  $9.439 \times 10^{-5}$  watt for the angle difference of 0 and 45 degree respectively. This angle difference represents the changes in the angular location of the Sun in the integrated end-to-end optical model.

Second, using the same conditions and the integrated optical model configuration, the incident flux arriving at the GOCI detector was simulated via ray tracing. The GOCI optical axis was set to point at 130E and 36N and the scan mirror direction was changed following the sequence shown in Fig. 7. In total, 106 rays were traced for the whole 16 tiles. The resulting flux values of  $1.198 \times 10^{-4}$  watt and  $6.384 \times 10^{-5}$  watt from the tile 10 were obtained for the angle difference of 0 and 45 degrees respectively.

By substituting  $1.335 \times 10^{-4}$  watt and  $9.439 \times 10^{-5}$  watt for Y and  $1.198 \times 10^{-4}$  watt and  $6.384 \times 10^{-5}$  watt for X in equation 2, it becomes a pair of solvable simultaneous linear equations. Solving the equation yields  $a = 0.6992$  and  $b = 4.975 \times 10^{-5}$  that serve as the flux correction factors between the detector plane and the entrance aperture. Fig. 7 shows all 16 tiles as seen by the detector, but with the flux correction coefficient via the method described in this section.

$$Y = a \times X + b \quad \text{Eq. (2)}$$

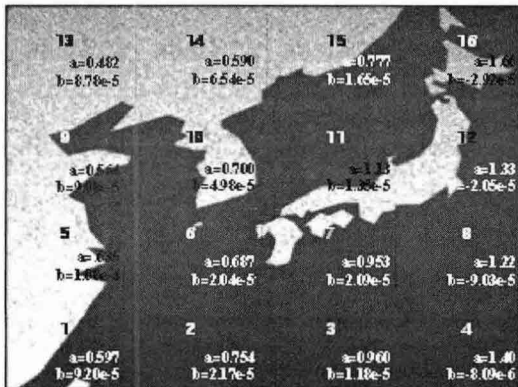


Fig. 7. Composite ray traced image around the Korean peninsula as seen by the detector. The number on the bottom left of each slot denotes GOCI scanning sequence. The flux correction coefficients for each measurement tile appear in the bracket. The ocean surface of 0.055 in reflectivity is darker than the land of 0.3 in reflectivity.

### 3.2. Demonstration of red tides detection

The method described in the previous section gives confidence that the end-to-end ray tracing and the GOCI optical system can be employed successfully to estimate the reflectance change from the ocean surface typically caused by the red tide. First, the coupled ocean atmosphere radiative transfer (COART) model[10] was used with the Chlorophyll concentration of up to 10 mg/m<sup>3</sup> at 443 nm wavelength. This represents the existence of the red tide infection, yielding the reflectivity (albedo) decrease from 0.055 (for normal sea water) to 0.041 around the south - east coastal area as seen in Fig. 8.

The end-to-end ray tracing was then used to compute the flux at the detector plane and it was then converted to the incident flux at the GOCI entrance aperture using the correction coefficients obtained from the relevant observation tile in Fig.7. The red tide infected area of about  $3.7 \times 10^4$  km<sup>2</sup> near the south - east corner of the Korean peninsular, shown in Fig. 8b, was obtained by subtracting the image of clear water from the red tide infected image. It is clearly observed that the red tide results in the flux reduction of about  $8.043 \times 10^{-7}$  watt in the relative flux unit. This proves the usefulness of the integrated end-to-end optical ray tracing model, reported here, for predicting the coastal water environment via the GOCI optical system.

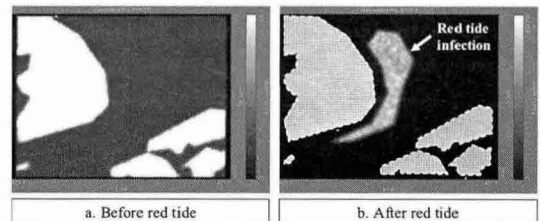


Fig. 8. Two images obtained with and without red tide. Chlorophyll concentration in the red tide is set to 10 mg/m<sup>3</sup> that tends to reduce the ocean reflectivity down to

0.041 at 443 nm wavelength following the COART model [10].

## 4. Conclusions

As a part of the GOCI development, we report the construction of a new integrated end-to-end optical ray tracing model including the sun (light source), the earth (observation target) and the GOCI optical system (observing instrument), all in one ray tracing environment. Using the model, we demonstrated its potential usefulness, whilst in a limited sense of first order approximation and in the relative flux unit, for the ground calibration and in-orbit performance verification such as red tide detection. Currently, the further refinement of the model and in computational robustness is progressing with the goal of full deployment at commencement of the ground calibration phase.

## Reference

- [1] C. R. Nagaraja Rao and Z. C. Nian, "Inter-calibration of meteorological satellite sensors in the visible and near-infrared", American Geostationary union, 2001, Vol. 28, No. 1, pp3-10.
- [2] G. Levrini and E. Attema, "The ENVISAT calibration and validation approach", ESA document PO-PL-ESA\_GS-1092
- [3] J. Xingwei, L. Mingsen and L.Jiangqiang, ", HY-1 satellite and its application in China", Proc. ACRS2004, New Generation Sensors and Applications.
- [4] M. Abbott and C. Davis, "Monitoring the coastal ocean with the GOES-R hyperspectral environmental suite coastal waters imager", NOAA document whitepaper.
- [5] GOCI engineering team, "GOCI design review report", Astrium document, 2005.
- [6] C. Bevilion, J.Archer et al., CodeV files, "TMA\_GOCI\_ss\_GLB\_150306.seq"
- [7] ASAP Primer 2005, Breault Research Organization
- [8] GOCI engineering team, "GOCI MTF model and performance", Astrium document, 2005.
- [9] ASAP online help, Breault Research Organization.
- [10] Jin, Z., T. Charlock, W. Smith Jr., and K Rutledge, "A parameterization of ocean surface albedo", Geophysical Research Letters, November 2004, L22301

## 저자

함 선 정(Sun-Jeong Ham)



2005년 2월 : 연세대학교 천문  
우주학과 졸업  
2005년 3월~현재 : 연세대학  
교 천문우주학과  
석사과정

<관심분야> 우주기기학, 광학, 원격탐사

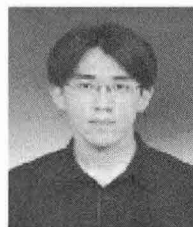
이 재 민(Jae-Min Lee)



2005년 2월 : 연세대학교  
자연과학부 졸업  
2005년 3월~현재 : 연세대학  
교 천문우주학과  
석사과정

<관심분야> 광학, 지구과학, 천문우주학

김 성 희 (Seonghui Kim)



2004년 2월 : 연세대학교  
천문우주학과 졸업  
2006년 2월 : 연세대학교  
천문우주학과 석사

<관심분야> 광학탐재체 설계

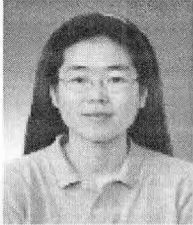
윤 형 식 (Heong Sik Youn)



1979.3~1983.2 광운대학교  
전기학 (학사)  
1983.8~1985.8 연세대학교  
전기학 (석사)  
1979.3~1983.2 연세대학교  
전기학(박사)

<관심분야> 광학탐재체 설계

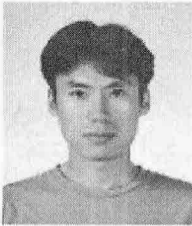
강 금 실(Gm Sil Kang)



1991.3.1~1995.2.28 제주대학  
교 기전공학(학사)  
1995.3.1~1997.2.28 광주과기  
대 기전공학(석사)  
1997.3.1~2004.2.28 광주과기  
대 기전공학(박사)

<관심분야> 광학탐재체 설계

명 환 춘(Hwan Chun Myung)



1991.3-1995.2 연세대학교  
전기공학 (학사)  
1995.3-1997.2 한국과학기술원  
전기전자(석사)  
1997.3-2002.8 한국과학기술원  
전기전자공(박사)

<관심분야> 광학탐재체 설계

김 석 환(Sug-Whan Kim)



1981년 2월 : 연세대학교  
천문기상학과 졸업  
1983년 월 : 연세대학교  
천문기상학과 석사  
1983년 10월~ 1993년 10월 :  
천문연구원 연구원  
1993년 10월 : 런던대학교  
천문기기 박사

1993년 10월~1999년 4월 : 런던대학교 광학연구소  
기술개발연구부장  
1999년 도월~2002년 2월 : 캘리포니아공과대학교  
교환교수  
1999년 5월~2002년 2월 : NASA JPL 비상주  
연구원  
2002년 3월~현재 : 연세대학교 천문우주학과정  
교수

<관심분야> 광학, 천문학 및 천체물리, 기계시스템,  
계측 및 제어